

Synthesis, X-ray crystal structure, NMR characterization and theoretical calculations on $[\text{Cp}_2\text{Ta}(\eta^2\text{-H}_2)(\text{CO})]^+$, the first thermally stable group 5 dihydrogen complex

Sylviane Sabo-Etienne,^a Venancio Rodriguez,^a Bruno Donnadieu,^a Bruno Chaudret,^{*a} Hassna Abou el Makarim,^{†b} Jean-Claude Barthelat,^b Stefan Ulrich,^c Hans-Heinrich Limbach^c and Claude Moise^d

^a Laboratoire de Chimie de Coordination du CNRS, 205, route de Narbonne, 31077 Toulouse cedex 04, France. E-mail: chaudret@lcc-toulouse.fr

^b Laboratoire de Physique Quantique (CNRS UMR 5626) IRSAMC, Université Paul Sabatier, 118, route de Narbonne, 31062 Toulouse cedex 04, France

^c Institut für Chemie, Freie Universität, Berlin, Takustrasse 3, D-14195 Berlin, Germany

^d Laboratoire de Synthèse et d'Electrosynthèse Organométalliques, Université de Bourgogne, 6, Boulevard Gabriel, 21000 Dijon, France

Received (in Montpellier, France) 10th March 2000, Accepted 15th June 2000

First published as an Advance Article on the web 28th November 2000

Protonation of $\text{Cp}_2\text{TaH}(\text{CO})$ ($\text{Cp} = \text{C}_5\text{H}_5$, **1a**; $\text{C}_5\text{H}_4\text{Bu}^t$, **1b**) by $\text{HBF}_4 \cdot \text{Et}_2\text{O}$ at -78°C in CH_2Cl_2 affords $[\text{Cp}_2\text{TaH}_2(\text{CO})]\text{BF}_4$ (**2**, **3**) as mixtures of 2 isomers. The minor ones (**2a**, **2b**) contain the known *trans*-dihydride $[\text{Cp}_2\text{TaH}_2(\text{CO})]^+$ cations whereas the major ones (**3a**, **3b**) are $[\text{Cp}_2\text{Ta}(\eta^2\text{-H}_2)(\text{CO})]\text{BF}_4$, the first group 5 dihydrogen complexes. The crystal structure of the analogous complex **3a** · BARf_4 recorded at 120 K confirms the presence of the coordinated dihydrogen ligand, which displays an H–H separation of 1.09(2) Å in agreement with distances calculated from NMR data. Protonation of $\text{Cp}_2\text{TaH}_2(\text{SiMe}_2\text{Ph})$ by $(\text{Et}_2\text{O})_2 \cdot \text{HBARf}_4$ does not lead to an analogous silane derivative but to the new dinuclear complex $[(\text{Cp}_2\text{TaH}_2)_2(\mu\text{-H})](\text{BARf}_4)$. Variable temperature NMR studies were carried out on the dihydrogen complex $[\text{Cp}_2\text{Ta}(\text{H}_2)(\text{CO})]^+$ (**3**) and its isotopomers. The high field signal of $[\text{Cp}_2\text{Ta}(\text{HD})(\text{CO})]^+$ (**3-d**) shows a decoalescence at 208 K in both ^1H and ^2D NMR, which allows us to calculate the barrier to rotation of HD (9.6 kcal mol⁻¹). The absence of decoalescence in the signal of **3** down to 173 K and the absence of a large kinetic isotope effect for the classical rotation of H_2 were demonstrated. These results are understood in terms of the presence of very large exchange couplings in a non-rotating dihydrogen ligand. The large barrier of rotation for the dihydrogen ligand in **3** was shown by DFT calculations to arise from a transition state in which the dihydrogen ligand is only coordinated through σ -donation from the H–H bond. The analogous phosphite and phosphine complexes $\{\text{Cp}_2\text{TaH}_2[\text{P}(\text{OMe})_3]\}^+$ (**4**) and $[\text{Cp}_2\text{TaH}_2(\text{PMe}_2\text{Ph})]^+$ (**5**) were shown to be *cis* dihydrides, in agreement with DFT calculations on a model compound, to display exchange couplings in NMR and no isotope effect for the classical exchange of the hydride ligands.

In the mid-eighties two major events renewed the interest in the interaction between dihydrogen and a transition metal. The most important was the discovery by Kubas and coworkers that dihydrogen can coordinate to a transition metal without being dissociated.^{1,2} The chemistry of dihydrogen complexes has developed very rapidly since then.^{2–7} Stable dihydrogen complexes were isolated for metals of groups 6–10 and a dihydrogen adduct of group 11 was observed in a matrix.⁵ As far as the chemistry of group 5 dihydrogen derivatives is concerned, in addition to the tantalum complexes discussed in this paper and the corresponding niobium derivatives (*vide infra*), the unstable complexes $\text{CpV}(\text{CO})_3(\eta^2\text{-H}_2)^{\text{8a}}$ and $\text{CpNb}(\text{CO})_3(\eta^2\text{-H}_2)^{\text{8b}}$ were characterized in a matrix whereas the corresponding tantalum complex was shown to be a classical dihydride.

Besides this major discovery, another new phenomenon was reported by two groups, namely the existence of large temperature-dependent H–H couplings in the ^1H NMR spectra of some transition metal polyhydrides.^{9,10} These couplings were rationalized in terms of quantum mechanical exchange.¹¹ The quantum mechanical origin of these coup-

lings was independently recognized by Zilm *et al.*¹² and by Weitekamp and coworkers,¹³ whereas the involvement of rotational tunneling was first proposed by Limbach *et al.*¹⁴ The existence and magnitude of the couplings were shown to be favoured by a reduction of the electronic density on the metal as was the formation of the dihydrogen state, which suggested a link between these two phenomena. Indeed, in the two similar complexes Cp_2NbH_3 and Cp_2TaH_3 displaying very different spectroscopic properties, calculations showed that the difference between their electronic structures was the existence of a low-lying dihydrogen state in the former.¹⁵

In both cases group 5 polyhydrides were involved. Thus, the spectroscopic properties of the above mentioned niobium complex Cp_2NbH_3 , characterized by two broad peaks in a 2 : 1 ratio, appeared puzzling¹⁶ and, as early as the 70's, during the course of reactivity studies, Tebbe and Parshall^{16a} observed that addition of AlEt_3 to Cp_2NbH_3 gave products with large H–H coupling constants (>100 Hz), which were not explained at that time but are now understood in terms of quantum mechanical exchange couplings.¹¹ The cationic tantalum dihydrides¹⁷ $[\text{Cp}_2\text{TaH}_2\text{L}]^+$ [$\text{L} = \text{P}(\text{OMe})_3$, PMe_2Ph] incorporating phosphine or phosphite ligands also displayed large H–H coupling constants, which were later demonstrated to be due to quantum mechanical exchange couplings.¹⁸ This

† Permanent address: Laboratoire de Chimie Théorique, Faculté des Sciences, Avenue Ibn Batouta, BP 1014, Rabat, Morocco.

led us to attempt the preparation of *cis*-dihydride complexes containing better π -accepting ligands in the equatorial plane in order to obtain larger exchange couplings and/or stabilize tantalum dihydrogen complexes. For this purpose, CO was first chosen since $\text{Cp}_2\text{TaH}(\text{CO})$ (**1**) is a readily accessible complex. *trans*- $[\text{Cp}_2\text{TaH}_2(\text{CO})]\text{PF}_6$ had previously been obtained by protonation of $\text{Cp}_2\text{TaH}(\text{CO})$ in aqueous HCl at room temperature.¹⁹ However precedents, in particular in ruthenium chemistry, have shown that low temperature protonation could lead to kinetic *cis*-isomers, which would adopt a dihydrogen configuration.²⁰ This led to the synthesis of *cis*- $[\text{Cp}_2\text{Ta}(\text{H}_2)(\text{CO})]\text{BF}_4$ (**3**), the first thermally stable group 5 dihydrogen complex.²¹ A similar chemistry carried out with niobium led to the dihydrogen complexes *cis*- $[\text{Cp}_2\text{Nb}(\text{H}_2)(\text{L})]^+$, but this time with better donor ligands such as phosphines, phosphites and isocyanides, the carbonyl complex being unstable.^{22,23} This result is in agreement with the fact that third row transition metals will have a greater tendency to dissociate H_2 because of stronger M–H bonds and better overlap between the metal and dihydrogen orbitals and therefore will need better π -acceptors to accommodate H_2 . Finally, the protonation of Cp_2NbH_3 in the presence of various ligands has recently been reported to lead to the *trans* dihydride derivatives $[\text{Cp}_2\text{NbH}_2(\text{L})]^+$.²⁴

We report in this paper full experimental details on the synthesis of cationic *cis*-tantalum dihydride complexes $[\text{Cp}_2\text{Ta}(\text{H}_2)(\text{L})]^+$ [$\text{L} = \text{CO}, \text{PMe}_2\text{Ph}, \text{P}(\text{OMe})_3$] and spectroscopic characterization of the complexes, including the demonstration of the hindered rotation of dihydrogen and of its relation with quantum mechanical exchange couplings. A significant part of this work has been reported in a preliminary form.^{18,21,25} We now report the X-ray crystal structure of $[\text{Cp}_2\text{Ta}(\text{H}_2)(\text{CO})]\text{BARf}_4$ { $\text{BARf}_4 = \text{B}[\text{C}_6\text{H}_3(\text{CF}_3)_2]_4$ }, the first crystal structure of a group 5 dihydrogen complex, protonation of related species and new calculations using the DFT/B3LYP method on the full system.

Results and discussion

Dihydrogen carbonyl complexes

Protonation of $\text{Cp}_2\text{TaH}(\text{CO})$ ($\text{Cp} = \text{C}_5\text{H}_5$, **1a**;¹⁹ $\text{C}_5\text{H}_4\text{Bu}^t$, **1b**) by stoichiometric amounts of $\text{HBF}_4 \cdot \text{Et}_2\text{O}$ in CH_2Cl_2 at -78°C affords rapidly $[\text{Cp}_2\text{TaH}_2(\text{CO})]\text{BF}_4$ as two isomeric classes of compounds (see Scheme 1). The minor isomers were identified by their spectroscopic properties as *trans*-

$[\text{Cp}_2\text{TaH}_2(\text{CO})][\text{BF}_4]$ (**2a**· BF_4 , **2b**· BF_4) similar to the complex previously characterized by one of us.¹⁹ The major isomers (**3a**· BF_4 , **3b**· BF_4) display a broad resonance at $\delta -4.98$ and $\delta -3.51$ at 293 K, respectively, which only broadens down to 178 K. The ratios **2a** : **3a** and **2b** : **3b** are 1 : 17 and 1 : 7, respectively. They remain constant throughout the temperature range observed and even after keeping the samples for 3 h at room temperature. The relaxation time T_1 of the hydrides (250 MHz, CD_2Cl_2) shows a minimum of 350 ms for **2a** and 9 ms for **3a** at 178 K and of 205 ms for **2b** and 12 ms for **3b** at 178 K, in agreement with the formulation of complexes **2a** and **2b** as classical dihydrides and **3a** and **3b** as dihydrogen derivatives. The latter are the first reported group 5 dihydrogen complexes. Evaluation of the H–H distance within the dihydrogen complexes **3a** and **3b** can be achieved using T_1 relaxation data. The relaxation time of metal bound hydrides (R_T), obtained in our case from measurements through the inversion/recovery method, is the sum of the relaxation due to hydride–hydride interaction ($R_{\text{H-H}}$) and of that due to all other phenomena (R_O , the relaxation due to dipole–dipole interactions with Cp, solvent, Ta, etc.).²⁶ $R_{\text{H-H}}$ can be neglected for **2a** whereas R_O should be very similar or identical for both **2a** and **3a**. Therefore the equations are:

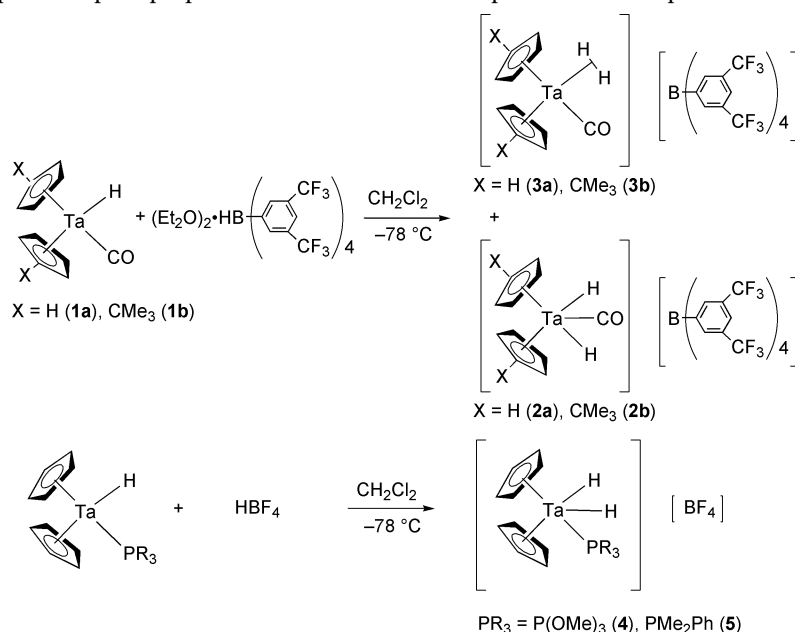
$$R_T(\mathbf{3a}) = R_{\text{H-H}}(\mathbf{3a}) + R_O(\mathbf{3a})$$

$$R_T(\mathbf{2a}) \approx R_O(\mathbf{2a}) \approx R_O(\mathbf{3a})$$

$$\Rightarrow R_{\text{H-H}}(\mathbf{3a}) = R_T(\mathbf{3a}) - R_T(\mathbf{2a})$$

This is a rare case where the relaxation due to the hydride–hydride interaction can be estimated with precision. Since we know that the dihydrogen molecule is blocked at low temperature, an approximate equation²⁶ allows us to calculate an H–H separation of $1.06 \pm 0.05 \text{ \AA}$ for **3a** and $1.12 \pm 0.05 \text{ \AA}$ for **3b**. These distances are in agreement with the presence of stretched dihydrogen ligands in the coordination sphere of tantalum. This was unexpected for a cationic early transition metal complex but is in agreement with the good electronic transfer from tantalum, a third row transition metal. It is interesting to note the variation of the relaxation time of the hydride signals of both isomers when substituting C_5H_5 by $\text{C}_5\text{H}_4\text{Bu}^t$. This is due to the variation of the electronic properties of the Cp ligands: the more electron-releasing ligand $\text{C}_5\text{H}_4\text{Bu}^t$ induces a lengthening of the H–H bond.

Upon carrying out the protonation of **1a** with $\text{DBF}_4 \cdot \text{D}_2\text{O}$, the expected 1 : 1 : 1 triplet centred at $\delta -5.18$ (see Fig. 1) was



Scheme 1 Protonation reactions of $\text{Cp}_2\text{TaH}(\text{CO})$ and $\text{Cp}_2\text{TaH}(\text{PR}_3)$ [$\text{PR}_3 = \text{P}(\text{OMe})_3, \text{PMe}_2\text{Ph}$].

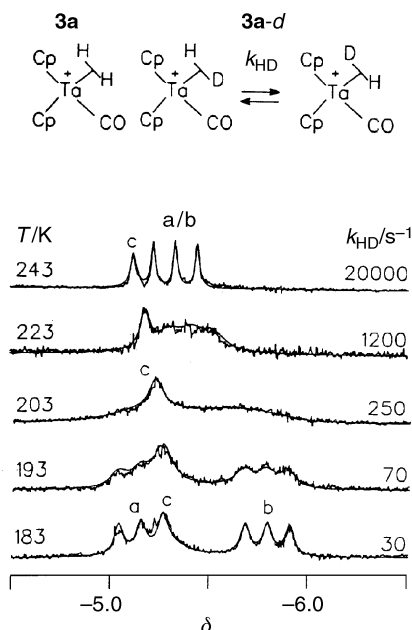


Fig. 1 High-field ^1H NMR spectra of $[\text{Cp}_2\text{Ta}(\text{HD})(\text{CO})]^+$ (**3a-d**) at various temperatures (250 MHz, CD_2Cl_2). Signal “c” represents the dihydrogen ligand of **3a**; signals “a” and “b” are for the *endo* and *exo* isomers of **3a-d**.

observed for **3a-d**, namely $[\text{Cp}_2\text{Ta}(\eta^2\text{-HD})(\text{CO})][\text{BF}_4]$. The $J_{\text{H-D}}$ value is 27.5 Hz in agreement with a dihydrogen structure. Using the correlation established by Morris *et al.*²⁷ or that of Luther and Heinekey,²⁸ it is possible to estimate the H–H distance knowing the H–D coupling within a dihydrogen complex. The value obtained is 0.96 Å, in fair but not excellent agreement with T_1 calculations. Upon lowering the temperature, the 1 : 1 : 1 triplet signal observed for the hydride coupled to the deuteride at $\delta -5.17$ ($J_{\text{H-D}}$ 27.5 Hz) coalesced at 208 K and transformed into two triplets at $\delta -5.78$ and $\delta -5.14$ ($J_{\text{H-D}}$ 27.5 Hz for both) due to the non-rotating HD molecule in which the hydrogen atom is located either next to CO or opposite to it. The energy of activation for the rotation of HD was calculated to be 9.6 kcal mol⁻¹ (see Fig. 1). This value is high and was unexpected for the rotation barrier of a coordinated HD molecule. It seems, however, typical for group 5 dihydrogen complexes since the barrier found for the niobium complexes $[\text{Cp}_2\text{Nb}(\text{HD})(\text{PMe}_2\text{Ph})]^+$ ²² and $[\text{Cp}_2\text{Nb}(\text{HD})(\text{NCR})]^+$ ($R = \text{Bu}^t, \text{Cy}, 2,6\text{-Me}_2\text{C}_6\text{H}_3$)²³ are respectively 11.0 and 10.0 kcal mol⁻¹.

It is surprising, however, that no decoalescence is observed for the high-field signal of **3a**, **b**. Two explanations could account for this observation: (i) a large kinetic isotope effect or (ii) very large couplings between the hydrogens of the coordinated dihydrogen molecule. In the latter case, when the H–H coupling constant J becomes large compared to the chemical shift difference $\Delta\nu$ ($J/\Delta\nu > 10$), the expected AB type spectrum would collapse into a single line located at a chemical shift intermediate between that of the hydrogen atoms. The determination of the individual chemical shifts of the hydrogens located respectively next to the carbonyl group or opposite to the carbonyl group was made possible by the decoalescence of the high-field signal of the HD isotopomer. In an experiment carried out at 250 MHz, $\Delta\nu = 160$ Hz and therefore the coupling between the hydrogens must be larger than 1600 Hz at 173 K. However, the same experiment was carried out in a freon mixture at 130 K and 500 MHz. Since no decoalescence was again observed this gives a minimum value of the H–H coupling constant of 3200 Hz at 130 K.

The ^2D NMR spectra (CD_2Cl_2 , 61.422 MHz) of a mixture of **3a-d** and $[\text{Cp}_2\text{Ta}(\text{D}_2)(\text{CO})]^+$ (**3a-d**₂) show at 298 K the presence of a signal attributed to coordinated D_2 at -5.67

ppm, which remains as a singlet down to 183 K. The signal for coordinated HD is not very clear on the spectrum but can easily be visualized using the INEPT $^2\text{D}/^1\text{H}$ technique. A doublet is observed at -5.07 ppm ($J_{\text{H-D}}$ ca. 27.5 Hz) at 298 K, which splits at 183 K into two doublets at -5.10 and -5.75 ppm. This demonstrates the decoalescence of the HD signal as observed by ^2D NMR. The presence of a single high-field line for **3a** (^1H NMR) and **3a-d**₂ (^2D NMR) and of a decoalescence for **3a-d** (^1H and ^2D NMR) cannot be attributed to a kinetic HH/HD/DD isotope effect since **3a-d**₂ would be expected to show a similar behaviour as **3a-d** but at higher temperature. These experiments therefore demonstrate the presence of very large H–H (D–D) couplings in $[\text{Cp}_2\text{Ta}(\text{H}_2)(\text{CO})]^+$ and $[\text{Cp}_2\text{Ta}(\text{D}_2)(\text{CO})]^+$. The origin of these couplings is quantum mechanical in nature and involves rotational tunneling of the coordinated dihydrogen ligand. Tunneling is possible for two similar particles but not for different ones such as H and D, hence explaining the decoalescence observed for the HD isotopomer.

In order to obtain crystals of these new complexes, the protonation of **1** was carried out under conditions similar to those used for the NMR studies (-78°C , CH_2Cl_2) but with $(\text{Et}_2\text{O})_2 \cdot \text{HBArf}_4$ [$\text{Arf} = (\text{CF}_3)_2\text{C}_6\text{H}_3$].²⁹ Addition of pentane to the reaction solution leads to the crystallization of the dihydrogen complexes (**3a** · BArf_4 , **3b** · BArf_4) in good yields (ca. 60%).

The crystal structure of **3a** · BArf_4 was solved by X-ray diffraction at 120 K and converged to a satisfactory agreement factor ($R = 0.052$ and $R_w = 0.062$). It consists (see Fig. 2 and Tables 1 and 2) of a classical “sandwich” structure with the carbonyl and dihydrogen ligands lying in the equatorial plane. The Ta–C and C–O distances within the coordinated carbonyl group are respectively 2.063(12) and 1.127(13) Å, slightly but not significantly longer than those found for **1** [respectively 1.94(4) and 1.21(4) Å], in agreement with the cationic nature of **3a** · BArf_4 .³⁰ Similarly, the Ta–H distances [1.78(4) and 1.81(4) Å] are longer in the present case than in **1** (1.45 Å, fixed value), as expected for a dihydrogen complex, and the H–H distance [1.09(2) Å] matches well the spectroscopic data. In particular this H–H distance is in agreement with the stretching of the H–H bond.

Tantalum dihydride complexes containing phosphorus donor ligands

The corresponding complexes incorporating phosphorus donor ligands [PMe_2Ph and $\text{P}(\text{OMe})_3$] had been previously

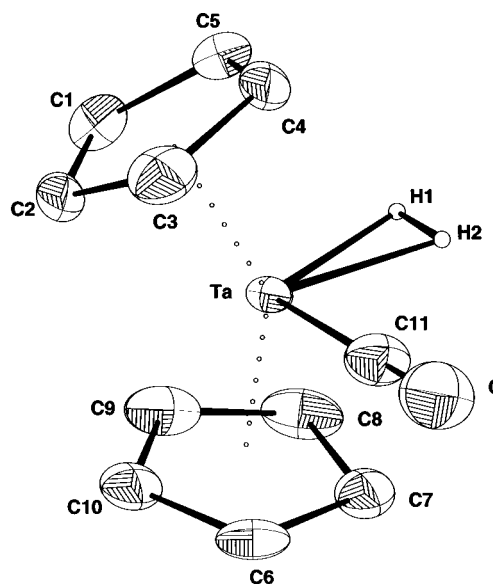


Fig. 2 Molecular structure of **3a** · BArf_4 with 50% probability ellipsoids for the non-hydrogen atoms.

Table 1 Crystal data, data collection and structure refinement of **3a** · BArf₄ · 1.5CH₂Cl

Chemical formula	[C ₁₁ H ₁₂ OTa][B(C ₆ H ₃ (CF ₃) ₂) ₄ · 1.5CH ₂ Cl ₂
Molecular weight	1331.77
Crystal system	Monoclinic
Space group	<i>P</i> 2 ₁ / <i>n</i>
<i>a</i> /Å	13.152(2)
<i>b</i> /Å	18.720(3)
<i>c</i> /Å	20.918(3)
β /°	99.40(2)
<i>U</i> /Å ³	5067(2)
<i>Z</i>	4
<i>T</i> /K	120
μ /cm ⁻¹	24.16
No of measured reflections	39 337
No of independent reflections	7545
Merging <i>R</i> value	0.044
<i>R</i>	0.052
<i>R</i> _w	0.062

prepared by Moise *et al.*¹⁷ The *cis*-dihydrides were prepared by protonation of the corresponding monohydrides (see Scheme 1) and shown to exhibit quantum mechanical exchange couplings, low in magnitude and of the same sign as the magnetic ones, in contrast to similar trihydride systems.¹⁸ For example, in the case of *cis*-{Cp₂TaH₂[P(OMe)₃]}⁺ (**4**), the couplings were found to vary between 76.1 Hz at 293 K and 12.5 Hz at 178 K, whereas for the phosphine complex *cis*-[Cp₂TaH₂(PMe₂Ph)]⁺ (**5**), they vary between 15.6 Hz at 310 K and 4.6 Hz at 193 K. The values of the different couplings are clearly related to the respective σ -donor and π -acceptor abilities of the different ligands. This point will be developed in the theoretical section of the present paper. However, having demonstrated that large H–H couplings rather than a kinetic isotope effect is at the origin of the apparent absence of decoalescence of the high-field signal of **3**, it was of interest to determine if the absence of kinetic isotope effect is a general property of such dihydrides. We therefore measured the ¹H NMR spectra of **4** and its isotopomer **4-d** at variable increasing temperatures. Two high-field signals are observed in ¹H NMR at room temperature (dioxane-*d*₈, 250 MHz; see Fig. 3) corresponding to the localization of the hydride either next to the phosphite ligand or opposite to it, respectively at δ –2.10 (*J*_{P–H} 89.1 Hz) and –0.94 (*J*_{P–H} 9.5 Hz). The *J*_{H–D} coupling constant was found to be *ca.* 1.5 Hz, in agreement with a classical dihydride formulation for *cis*-{Cp₂Ta(H)₂[P(OMe)₃]}⁺ (**4**), for which an H–H separation of 1.67 Å was calculated using *T*₁ minimum data (87 ms at 180 K, 250 MHz). The hydride signals for the isotopomers **4** and **4-d** both show a coalescence at the same temperature of about 360 K (250 MHz, dioxane-*d*₈), indicating the absence of a kinetic HH/HD isotope effect for the hydride/hydride exchange. The process is characterized by a barrier of 16.6

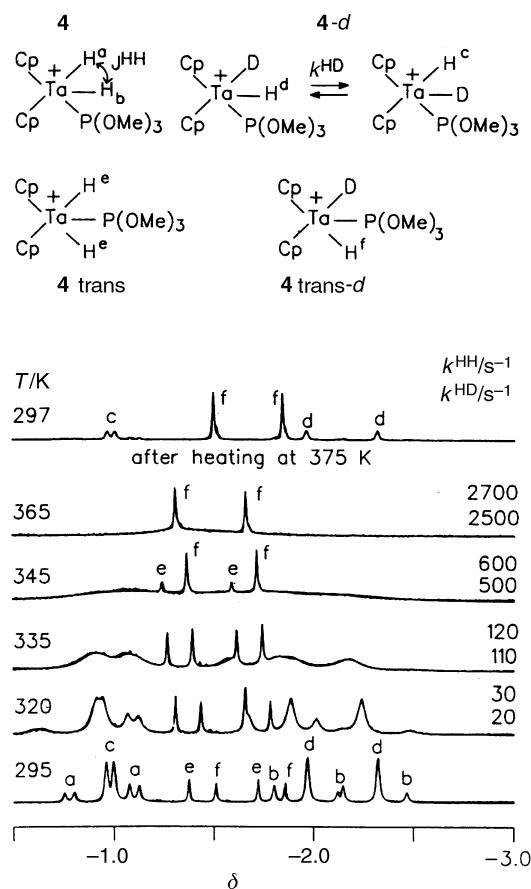
Table 2 Selected bond distances (Å) and angles (°) for **3a** · BArf₄ (esd's in parentheses refer to the last significant digit)^a

H(1)–H(2)	1.09(2)	Ta–H(1)	1.81(4)
Ta–H(2)	1.78(4)	Ta–C(1)	2.357(11)
Ta–C(2)	2.37(1)	Ta–C(3)	2.357(11)
Ta–C(4)	2.32(1)	Ta–C(5)	2.350(11)
Ta–C(6)	2.37(1)	Ta–C(7)	2.32(1)
Ta–C(8)	2.36(1)	Ta–C(9)	2.344(12)
Ta–C(10)	2.37(1)	Ta–C(11)	2.063(12)
O–C(11)	1.127(13)	Ta–L2	2.0358
Ta–L1	2.0305		
C(11)–Ta–H(2)	64.1(3)	C(11)–Ta–H(1)	98.9(3)
Ta–C(11)–O	179.2(1)	H(1)–Ta–H(2)	35.4(9)

^a L1 = centroid of C(1)–C(5), L2 = centroid of C(6)–C(10).

kcal mol⁻¹, as obtained by the lineshape analysis shown on Fig. 3. The spectra also show a slow transformation of **4** into the *trans* form, especially at high temperatures, probably linked to H/D exchange with the solvent and D₂O present in the reaction mixture through deprotonation/protonation processes since, after heating to 375 K and cooling, **4 trans-d** is the major isotopomer present in solution.

These results therefore confirm that (i) a classical fluxional process is operative in, so far, every system displaying quantum exchange and (ii) no kinetic isotope effect is present for the classical hydride/hydride exchange process.

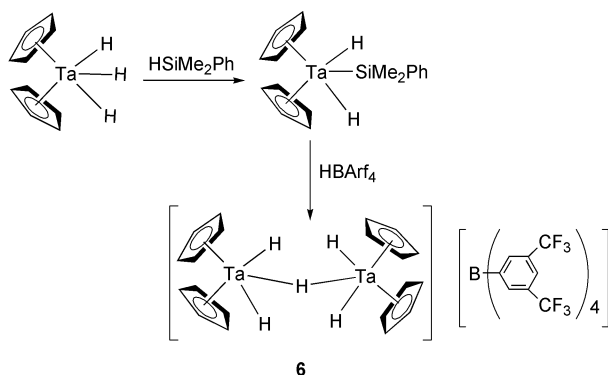
**Fig. 3** High-field ¹H NMR spectra of the mixture *cis*-{Cp₂Ta(H)₂[P(OMe)₃]}⁺ (**4**), *cis*-{Cp₂Ta(H)(D)[P(OMe)₃]}⁺ (**4-d**), *trans*-{Cp₂Ta(H)₂[P(OMe)₃]}⁺ (**4 trans**) and *trans*-{Cp₂Ta(H)(D)[P(OMe)₃]}⁺ (**4 trans-d**) at various temperatures (250 MHz, dioxane-*d*₈).

Protonation of a tantalum hydrido silyl complex

Since the protonation of **1** leads to a complex characterized as the first group 5 dihydrogen derivative, it was of interest to study other systems that could lead to other novel structures. The protonation of Cp_2TaH_3 ²⁴ could produce dihydrido dihydrogen or bis(dihydrogen) complexes while the protonation of $\text{Cp}_2\text{TaH}_2(\text{SiMe}_2\text{Ph})$ ³¹ could lead to a complex containing coordinated dihydrogen, coordinated silane or both. The reaction with Cp_2TaH_3 did not lead to a dihydrogen complex. However, protonation of $\text{Cp}_2\text{TaH}_2(\text{SiMe}_2\text{Ph})$ by $(\text{Et}_2\text{O})_2 \cdot \text{HBARf}_4$ yielded a new dinuclear complex $[(\text{Cp}_2\text{TaH}_2)_2(\mu\text{-H})](\text{BARf}_4)$ (**6**; Scheme 2), isolated as white crystals in good yield (59%). The ¹H NMR spectrum of this complex (200 MHz, CD_2Cl_2) shows an AX_4 type spectrum at high field: a quintet at -17.16 ppm (1H, $J_{\text{H-H}}$ 9.8 Hz) and a doublet at 0.82 ppm (4H), corresponding respectively to one bridging and four terminal hydrides. This indicates the formation of a dinuclear complex linked by only one bridging hydride. The mechanism of formation of this complex is unknown.

DFT calculations on $[\text{Cp}_2\text{TaH}_2\text{L}]^+$ with $\text{L} = \text{CO}, \text{PH}_3$

Four isomers have been located on the potential energy surface when $\text{L} = \text{CO}$. They are depicted in Fig. 4, and selected sets of optimized bond lengths and angles are listed in Tables 3 and 4. Isomers A, B and C have been found to be minima on the surface. The most stable point on the surface is isomer A with the carbonyl ligand lying in a central position. This isomer with C_{2v} symmetry is characterized by a distort-



Scheme 2 Protonation reaction of $\text{Cp}_2\text{TaH}_2(\text{SiMe}_2\text{Ph})$.

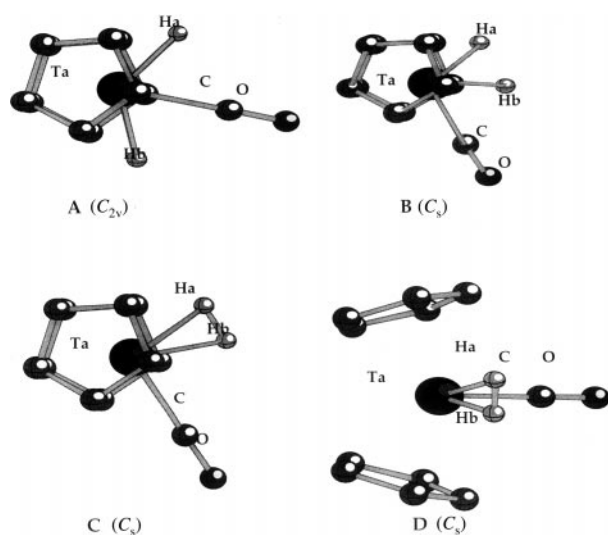


Fig. 4 Geometries of the stationary points located on the potential energy surface of $[\text{Cp}_2\text{TaH}_2(\text{CO})]^+$. Hydrogen atoms of the Cp ring are omitted for clarity.

Table 3 Optimized geometrical parameters for the *cis*- and *trans*- $[\text{Cp}_2\text{TaH}_2(\text{CO})]^+$ dihydride complexes.^a Distances are in Å and angles in °

	<i>trans</i> (A)		<i>cis</i> (B)	
	B3LYP	B3LYP	B3LYP	BLYP
Ta–H _a	1.759	1.735	1.750	
Ta–H _b	1.759	1.778	1.791	
H _a –H _b	3.191	1.504	1.516	
Ta–C	2.161	2.135	2.133	
C–O	1.142	1.146	1.160	
Ta–L ₁	2.110	2.131	2.138	
H _a –Ta–H _b	130.2	50.7	50.7	
H _a –Ta–C	65.1	113.3	113.0	
H _b –Ta–C	65.1	62.6	62.3	
L ₁ –Ta–L ₂	139.8	138.8	141.0	
Ta–C–O	180.0	176.6	179.9	

^a See Fig. 4 for labeling of the hydrides. L₁ and L₂ stand for the Cp centres.

tion of the *trans* equatorial hydride ligands, which are bent away from the Cp ligand with an H_a–Ta–H_b angle of 130.2°. A similar geometry with an H–Ta–H angle of 129.8° has been found at the MP2 level in the d⁰ complex $[\text{TaH}_2(\text{OH})_2(\text{CO})(\text{PH}_3)]^+$ by Bayse and Hall.³² The reason for this distortion is the strong π -acceptor property of the CO ligand, which polarizes the Ta d orbital used to coordinate the hydrides. The calculated Ta–H distance of 1.759 Å is typical of tantalum–hydride distances and compares very well with the MP2 value of 1.756 Å obtained in the previous complex.

Isomers B and C are of C_s symmetry with the two hydrogen atoms on the same side with respect to CO, in the equatorial plane. The characteristic geometrical feature of isomer B is the presence of two inequivalent Ta–H bonds with a distance between the two hydrides of 1.504 Å. It can therefore be described as a classical *cis*-dihydride complex. It can be noticed that the in-plane π^* CO orbital polarizes the two Ta–H bonds differently leading to one bond (Ta–H_a) being slightly shorter than in isomer A and the other (Ta–H_b) being slightly longer (by about 0.02 Å).

Isomer C is clearly a dihydrogen complex. The ($\eta^2\text{-H}_2$) coordination mode is confirmed by a significant lengthening of the H_a–H_b bond (0.922 Å vs. 0.74 Å in free dihydrogen), and Ta–H_a and Ta–H_b bond distances (1.834 and 1.858 Å, respectively) much longer than in isomer A and B. The optimized geometry of isomer C closely resembles that found by X-ray diffraction for $3\text{a} \cdot \text{BARf}_4$. As expected,³³ DFT calculations give metal–hydrogen bond distances that are too long. The H_a–H_b bond distance is calculated to be smaller than the

Table 4 Optimized geometrical parameters for the $[\text{Cp}_2\text{Ta}(\eta^2\text{-H}_2)(\text{CO})]^+$ complexes.^a Distances are in Å and angles in °

	Isomer C			Isomer D
	B3LYP	BLYP	EXP	B3LYP
Ta–H _a	1.834	1.842	1.81(4)	2.039
Ta–H _b	1.858	1.865	1.78(4)	2.039
H _a –H _b	0.922	0.940	1.09(2)	0.787
Ta–C	2.103	2.104	2.063(12)	2.078
C–O	1.151	1.165	1.127(13)	1.156
Ta–L ₁	2.102	2.165	—	2.091
H _a –Ta–H _b	28.9	29.4	35.4(9)	22.3
H _a –Ta–C	102.6	102.6	98.9(25)	90.5
H _b –Ta–C	73.3	73.2	64.1(26)	90.5
L ₁ –Ta–L ₂	140.1	140.2	—	140.6
Ta–C–O	179.1	179.9	179.2(11)	176.5

^a See Fig. 4 for labeling of the hydrides. L₁ and L₂ stand for the Cp centres.

X-ray experimental one by about 0.17 Å. The use of the non-hybrid functional BLYP does not alter this result. However, the H_a-H_b calculated value is in an overall good agreement with the values deduced from NMR experiments using T_1 data, and confirms an important stretching of the coordinated H–H bond.

The relative energies of the B3LYP-optimized geometries are presented in Table 5. The three isomers of $[Cp_2TaH_2(CO)]^+$ are within an energy range of 4 kcal mol⁻¹. Isomers A and C are separated by only 2.4 kcal mol⁻¹. They correspond to the two isomers **2a** and **3a** afforded by protonation of $Cp_2TaH(CO)$ and identified by NMR spectroscopy. This result is in agreement with experimental results demonstrating that **2a** is the thermodynamic isomer and **3a** the kinetic isomer.

Additionally, the transition state structure of the rotation of H_2 in isomer C was optimized by forcing the H_2 fragment to be perpendicular to the plane of symmetry of the molecule. This structure corresponds to isomer D in Fig. 4, and its structural parameters can be found in Table 4. The rotational barrier is calculated to be 12.7 kcal mol⁻¹, in good agreement with that obtained from NMR data (9.6 kcal mol⁻¹). This high value is due to the complete loss of back-donation from the metal centre into the σ^* orbital of H_2 in the rotated structure. This statement is corroborated by the change in the H–H distance, from 0.922 Å in isomer C to 0.787 Å in the transition structure, while the Ta–H bond lengths increase by about 0.2 Å.

For the phosphine complex $[Cp_2TaH_2(PH_3)]^+$, three stationary points of interest have been identified on the potential energy surface. The B3LYP-optimized geometries of three isomers are featured in Fig. 5, and a set of selected geometrical parameters can be found in Table 6. As for the carbonyl complexes, the most stable isomer A corresponds to a *trans*-

Table 5 Relative energies (in kcal mol⁻¹) of the various isomers of $[Cp_2TaH_2L]^+$ at the DFT/B3LYP level of calculation

	L = CO	L = PH ₃
Dihydride complexes		
<i>trans</i> (A)	0.0	0.0
<i>cis</i> (B)	4.0	9.8
η^2-H_2 complexes		
Coplanar (C)	2.4	—
Perpendicular (D)	15.1	25.8

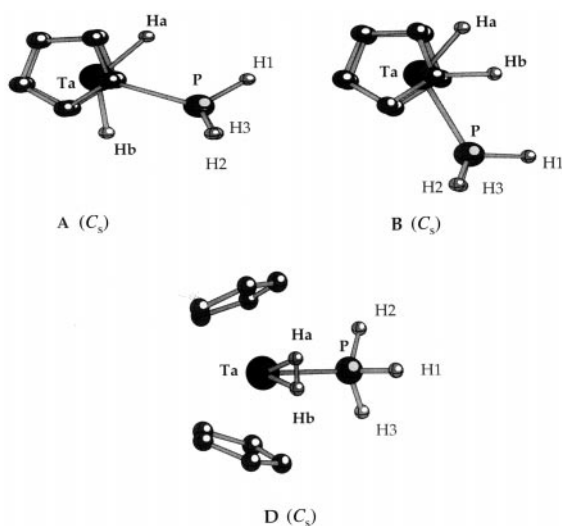


Fig. 5 Geometries of the stationary points located on the potential energy surface of $[Cp_2TaH_2(PH_3)]^+$. Hydrogen atoms of the Cp ring are omitted for clarity.

Table 6 Optimized geometrical parameters for $[Cp_2TaH_2(PH_3)]^+$ complexes.^a Distances are in Å and angles in °

	Dihydride complexes		η^2-H_2 complex
	<i>trans</i> (A)	<i>cis</i> (B)	Perpendicular (D)
Ta–H _a	1.751	1.724	2.045
Ta–H _b	1.763	1.762	2.045
H _a –H _b	3.191	1.584	0.787
P–H ₁	1.428	1.426	1.431
P–H ₂	1.431	1.431	1.440
Ta–L ₁	2.114	2.123	2.075
Ta–P	2.599	2.638	2.541
H ₂ –P–H ₃	98.2	97.7	99.0
H ₁ –P–H ₂	99.0	98.1	96.8
H _a –Ta–H _b	130.5	54.0	22.2
L ₁ –Ta–L ₂	138.2	138.3	141.1
H _a –Ta–P	62.3	119.3	88.5
H _b –Ta–P	68.2	65.2	88.5
L ₁ –Ta–P	111.0	105.0	105.7

^a See Fig. 5 for labeling of the hydrides. L₁ and L₂ stand for the Cp centres.

dihydride structure in which the hydride ligands bend toward the phosphine. The calculated value of the H_a-Ta-H_b bond angle (130.5°) is of the same order of magnitude as in the *trans*-dihydride carbonyl complex, indicating that the distortion of the hydrides is characteristic of the d-orbital occupancy of the metal. In contrast to the case with L = CO, the phosphine complex has only one isomeric form in which the two hydrides occupy a lateral position with respect to PH_3 . Isomer B can be formulated as a classical *cis*-dihydride with an H_a-H_b distance of 1.584 Å. This value is in good agreement with the H–H separation of 1.67 Å calculated from NMR data for *cis*- $[Cp_2TaH_2[P(OMe)_3]]^+$. The reason for the absence of an η^2-H_2 isomer in this compound is that the PH_3 ligand acts as a weak π -acceptor. Therefore, the delicate balance between L and H_2 for back-bonding is in favour of H_2 , which leads to the breaking of the H–H bond.

Finally, the barrier to hydride/hydride exchange in isomer B has been calculated by optimizing the geometry of the transition structure in which the H_2 fragment is perpendicular to the plane of symmetry (see isomer D in Fig. 5). This isomer displays the same geometrical features as the corresponding transition state in the carbonyl complex, that is a weakly bonded H_2 molecule. The height of the barrier is calculated to be 16.0 kcal mol⁻¹, in good agreement with the value of 16.6 kcal mol⁻¹ obtained by lineshape analysis for hydride/hydride exchange in complex **4**.

Conclusions

We report in this article the first X-ray crystal structure of a group 5 dihydrogen complex. The complex is formally d² but accommodates a stretched dihydrogen ligand, hence suggesting an efficient back-bonding from the metal. The dihydrogen ligand is very sensitive to small variations of the electron density on the metal as found experimentally and modelled by calculations. Thus, replacing CO by a phosphine ligand induces the formation of a *cis*-dihydride complex.

It has not been possible to extend this study to the preparation of the analogous silane complexes but the protonation of the dihydridosilyl complex has led to an interesting dinuclear tantalum derivative containing a single hydride bridge, $[(Cp_2TaH_2)_2(\mu-H)](BARf_4)$. This complex results formally from the coordination of Cp_2TaH_3 to the cationic $Cp_2TaH_2^+$ fragment and therefore can be viewed as another example of a σ -bond tantalum complex, in the present case a Ta–H bond.

The most original result of this work concerns the presence of quantum mechanical exchange couplings in

the *cis*-dihydride or dihydrogen derivatives. In $\{\text{Cp}_2\text{TaH}_2[\text{P}(\text{OMe})_3]\}^+$ (**4**), the exchange couplings result from the possibility of the two hydrogens to exchange through a dihydrogen transition state located 16 kcal mol⁻¹ above the ground state. This transition state is the same as that found for the dihydrogen rotation in the carbonyl complexes. In this transition state, the dihydrogen ligand is perpendicular to the equatorial plane and only coordinated through σ -donation from the H–H bond. This is clear when considering the H–H distance of 0.787 Å calculated for the transition state of the carbonyl complex. This absence of back-donation explains the height of the barrier (9.6 kcal mol⁻¹), which is very unusual for dihydrogen rotation and only observed in d² systems.

Experimental

Syntheses

[Cp₂Ta(H₂)(CO)]BARf₄ (3a). To a solution of Cp₂Ta(H)(CO) (75 mg, 0.22 mmol) in 4 mL of CH₂Cl₂ at –78 °C was added a solution of (Et₂O)₂ · HBARf₄ (222.6 mg, 0.22 mmol) in 1 mL of CH₂Cl₂ *via* canula. The reaction mixture was stirred for 30 min. Pentane (6 mL) was slowly added and diffused into the resulting yellow solution. After 2 days at –30 °C, the complex was isolated as yellow crystals. Yield: 60%. ¹H-NMR (200 MHz, CD₂Cl₂): δ 7.74 (br, 8H, H-*o* of BARf₄), 7.58 (s, 4H, H-*p* of BARf₄), 5.57 (s, 10H, C₅H₅), –5.05 [s, 2H, Ta(H₂)]. Anal. calc. for C₄₃H₂₄BF₂₄OTa: C 42.88, H 1.99; found: C 42.44, H 1.77%.

[(C₅H₄Bu^t)₂Ta(H₂)(CO)]BARf₄ (3b). To a solution of (C₅H₄Bu^t)₂Ta(H)(CO) (50 mg, 0.11 mmol) in 3 mL of CH₂Cl₂ at –78 °C was added a solution of (Et₂O)₂ · HBARf₄ (111.9 mg, 0.11 mmol) in 1 mL of CH₂Cl₂ *via* canula. The reaction mixture was stirred for 30 min. Pentane (5 mL) was slowly added and diffused into the resulting yellow solution. After 2 days at –30 °C, the complex was isolated as yellow crystals. Yield: 56%. ¹H-NMR (200 MHz, CD₂Cl₂): δ 7.72 (br, 8H, H-*o* of BARf₄), 7.57 (s, 4H, H-*p* of BARf₄), 5.67 (m, 2H, C₅H₄), 5.60 (m, 2H, C₅H₄), 5.40 (m, 2H, C₅H₄), 5.20 (m, 2H, C₅H₄), 1.24 (s, 18H, Bu^t), –4.01 [s, 2H, Ta(H₂)]. Anal. calc. for C₅₁H₄₀BF₂₄OTa: C 46.52, H 3.07; found: C 46.04, H 2.81%.

[(Cp₂TaH₂)₂(μ -H)]BARf₄ (6). To a solution of Cp₂TaH₂(SiMe₂Ph) (36 mg, 0.08 mmol) in 3 mL of CH₂Cl₂ at –78 °C was added a solution of (Et₂O)₂ · HBARf₄ (81.1 mg, 0.08 mmol) in 1 mL of CH₂Cl₂ *via* canula. The reaction mixture was stirred for 30 min. Pentane (5 mL) was slowly added and diffused into the resulting colourless solution. After resting overnight at –30 °C, the complex was isolated as white crystals. Yield: 59%. ¹H-NMR (200 MHz, CD₂Cl₂): δ 7.72 (br, 8H, H-*o* of BARf₄), 7.57 (s, 4H, H-*p* of BARf₄), 5.77 (s, 10H, C₅H₅), 0.82 (d, 4H, $J_{\text{HH}} = 9.3$, Ta–H), –17.16 [q, 1H, $J_{\text{HH}} = 9.8$ Hz, Ta(μ -H)]. Anal. calc. for C₅₂H₃₇BF₂₄Ta: C 41.89, H 2.51; found: C 41.25, H 2.27%.

X-Ray analysis of 3a · BARf₄ · 1.5CH₂Cl₂

Data collection were carried out at low temperature ($T = 120$ K) on a Stoe Imaging Plate Diffraction System (IPDS), equipped with an Oxford Cryosystems Cryostream cooler device and using graphite-monochromated Mo-K α radiation ($\lambda = 0.71073$ Å). Final unit cell parameters were obtained by least-squares refinement of a set of 5000 reflections, and crystal decay was monitored by measuring 200 reflections per image. No significant fluctuation of intensity was observed during data collection. Numerical absorption corrections³⁴ were applied on the data by using a set of symmetry equivalent reflections selected with the criterion [$I > 30\sigma(I)$] such that all directions of the reflection space were equally represented.

The structure was solved by direct methods SIR92,³⁵ and refined by least-squares procedures on F_{obs} (CRYSTALS).³⁶ All hydrogen atoms were located on a difference Fourier map, but they have been introduced in the calculation in idealized positions, with an isotropical thermal parameter fixed at 20% higher than those of the carbon to which they are bound. The hydrides H(1) and H(2) have been isotropically refined. All non-hydrogen atoms were anisotropically refined and in the last cycles of refinement using a weighting scheme. The drawing of the molecule is performed with CAMERON³⁷ with 50% probability displacement ellipsoids for non-hydrogen atoms.

CCDC reference number 440/202. See <http://www.rsc.org/suppdata/nj/b0/b002073g/> for crystallographic files in .cif format.

Computational details

All calculations were performed with the GAUSSIAN 98 program.³⁸ For tantalum, the core electrons were represented by a relativistic small-core pseudopotential derived using the Durand–Barthelat method.³⁹ The thirteen electrons corresponding to the 5s, 5p, 5d and 6s atomic orbitals were described by a (8s, 6p, 6d) primitive set of Gaussian functions contracted to [7s, 5p, 3d]. Standard pseudopotentials developed in Toulouse⁴⁰ were used to describe the atomic cores of all other atoms (P, C, O). A double-zeta plus polarization valence basis set was employed for each atom (d-type function exponents were 0.45, 0.80 and 0.85, respectively). For hydrogen, a primitive (4s) basis set contracted to [2s] was used. A p-type polarization function (exponent 0.9) was added for the two hydrogen atoms directly bound to tantalum (H_a and H_b).

All stationary points of interest were located at the B3LYP level of theory, a density functional theory (DFT) type of calculation based on hybrid functionals. Analytical first derivatives of the energy were used to optimize geometrical parameters and frequency calculations were performed to determine the nature of the stationary points.

Acknowledgements

This work was supported by the European Union, Brussels, *via* the Human Capital & Mobility Network “Localization and Transfer of Hydrogen”, the Deutsche Akademische Austauschdienst, Bonn-Bad Godesberg, within the programme PROCOPE (H.-H. L., B. C.), the CNRS (B. C., S. S.-E.) and the Fonds der Chemischen Industrie, Frankfurt (S. U., H.-H. L.). The authors thank Madame Perret for technical assistance.

References

- G. J. Kubas, R. R. Ryan, B. I. Swanson, P. J. Vergamini and H. J. Wasserman, *J. Am. Chem. Soc.*, 1984, **100**, 451.
- G. J. Kubas, *Acc. Chem. Res.*, 1988, **21**, 120.
- (a) R. H. Crabtree, *Acc. Chem. Res.*, 1990, **23**, 95; (b) R. H. Crabtree, *Angew. Chem., Int. Ed. Engl.*, 1993, **32**, 789.
- P. G. Jessop and R. H. Morris, *Coord. Chem. Rev.*, 1992, **121**, 155.
- D. M. Heinekey and W. J. Oldham, Jr., *Chem. Rev.*, 1993, **93**, 913.
- D. G. Gusev, J. U. Notheis, J. R. Rambo, B. E. Hauger, O. Eisenstein and K. G. Caulton, *J. Am. Chem. Soc.*, 1994, **116**, 7409.
- S. Sabo-Etienne and B. Chaudret, *Coord. Chem. Rev.*, 1998, **178–180**, 381.
- (a) M. T. Haward, M. W. George, S. M. Howdle and M. Poliakoff, *J. Chem. Soc., Chem. Commun.*, 1990, 913; (b) M. T. Haward, M. W. George, P. Hamley and M. Poliakoff, *J. Chem. Soc., Chem. Commun.*, 1991, 1101.
- (a) T. Arliguie, B. Chaudret, J. Devillers and R. Poilblanc, *C. R. Séances Acad. Sci., Ser. 2*, 1987, **305**, 1523; (b) A. Antinolo, B. Chaudret, G. Commenges, M. Fajardo, F. Jalon, R. H. Morris, A. Otero and C. T. Schweitzer, *J. Chem. Soc., Chem. Commun.*, 1988, 1210.
- D. M. Heinekey, N. G. Payne and G. K. Schulte, *J. Am. Chem. Soc.*, 1988, **110**, 2303.

- 11 S. Sabo-Etienne and B. Chaudret, *Chem. Rev.*, 1998, **98**, 2077.
- 12 (a) K. W. Zilm, D. M. Heinekey, J. M. Millar, N. G. Payne and P. Demou, *J. Am. Chem. Soc.*, 1989, **111**, 3088; (b) D. M. Heinekey, J. M. Millar, T. F. Koetzle, N. G. Payne and K. W. Zilm, *J. Am. Chem. Soc.*, 1990, **112**, 909; (c) K. W. Zilm, D. M. Heinekey, J. M. Millar, N. G. Payne, S. P. Neshyba, J. C. Duchamps and J. Szczyrba, *J. Am. Chem. Soc.*, 1990, **112**, 920.
- 13 D. H. Jones, J. A. Labinger and D. P. Weitekamp, *J. Am. Chem. Soc.*, 1989, **111**, 3087.
- 14 (a) H.-H. Limbach, M. Maurer, G. Scherer and B. Chaudret, *Angew. Chem., Int. Ed. Engl.*, 1992, **31**, 1369; (b) H.-H. Limbach, S. Ulrich, G. Buntkowski, S. Sabo-Etienne, B. Chaudret, G. J. Kubas and J. Eckert, *J. Am. Chem. Soc.*, 1998, **120**, 7929.
- 15 (a) J. C. Barthelat, B. Chaudret, J. P. Daudey, P. De Loth and R. Poilblanc, *J. Am. Chem. Soc.*, 1991, **113**, 9896; (b) S. Camanyes, F. Maseras, M. Moreno, A. Lledos, J. M. Lluch and J. Bertran, *J. Am. Chem. Soc.*, 1996, **118**, 4617.
- 16 (a) F. N. Tebbe and G. W. Parshall, *J. Am. Chem. Soc.*, 1971, **93**, 3793; (b) J. A. Labinger, *Comp. Organomet. Chem.*, 1982, **3**, 707.
- 17 J.-F. Leboeuf, O. Lavastre, J.-C. Leblanc and C. Moïse, *J. Organomet. Chem.*, 1991, **418**, 359.
- 18 B. Chaudret, H.-H. Limbach and C. Moïse, *C. R. Séances Acad. Sci., Ser. 2*, 1992, **315**, 533.
- 19 J. F. Reynoud, J.-F. Leboeuf, J.-C. Leblanc and C. Moïse, *Organometallics*, 1986, **5**, 1863.
- 20 M. S. Chinn and D. M. Heinekey, *J. Am. Chem. Soc.*, 1990, **112**, 5166.
- 21 S. Sabo-Etienne, B. Chaudret, H. Abou El Makarim, J. C. Barthelat, J. P. Daudey, C. Moïse and J. C. Leblanc, *J. Am. Chem. Soc.*, 1994, **116**, 9335.
- 22 F. A. Jalon, B. Manzano, A. Otero, E. Villasenor and B. Chaudret, *J. Am. Chem. Soc.*, 1995, **117**, 10123.
- 23 A. Antinolo, F. Carrillo-Hermosilla, M. Fajardo, S. Garcia-Yuste, A. Otero, S. Camanyes, F. Maseras, M. Moreno, A. Lledos and J. M. Lluch, *J. Am. Chem. Soc.*, 1997, **119**, 6107.
- 24 P. Sauvageot, A. Sadorge, B. Nuber, M. K. Kubicki, J.-C. Leblanc and C. Moïse, *Organometallics*, 1999, **18**, 2133.
- 25 S. Sabo-Etienne, B. Chaudret, H. Abou El Makarim, J. C. Barthelat, J. P. Daudey, S. Ulrich, H.-H. Limbach and C. Moïse, *J. Am. Chem. Soc.*, 1995, **117**, 11602.
- 26 M. T. Bautista, E. P. Capellani, S. D. Drouin, R. H. Morris, C. T. Schweitzer, A. Sella and J. P. Zbuckowski, *J. Am. Chem. Soc.*, 1991, **113**, 4876.
- 27 P. A. Maltby, M. Schlaf, M. Steinbeck, A. J. Lough, R. H. Morris, W. T. Klooster, T. F. Koetzle and R. C. Srivastava, *J. Am. Chem. Soc.*, 1996, **118**, 5396.
- 28 T. A. Luther and D. M. Heinekey, *Inorg. Chem.*, 1998, **37**, 127.
- 29 M. Brookhart, B. Grant and A. F. Volpe, Jr., *Organometallics*, 1992, **11**, 3920.
- 30 D. F. Foust, R. D. Rogers, M. D. Rausch and J. L. Atwood, *J. Am. Chem. Soc.*, 1982, **104**, 5646.
- 31 M. D. Curtis, L. G. Bell and W. M. Butler, *Organometallics*, 1985, **4**, 701.
- 32 C. A. Bayse and M. B. Hall, *Organometallics*, 1998, **17**, 4861.
- 33 See, for example: J. A. Ayllon, S. F. Sayers, S. Sabo-Etienne, B. Donnadiou, B. Chaudret and E. Clot, *Organometallics*, 1999, **18**, 3981.
- 34 X-SHAPE Crystal Optimisation for Numerical Absorption Correction, Revision 1.01, STOE and Cie GMBH, Darmstadt, 1996 (X-SHAPE is based on the program HABITUS by Dr. W. Herrendorf, Institut für Anorganische Chemie, Universität Giessen, Darmstadt, Germany.)
- 35 A. Altomare, G. Casciarano, G. Giacovazzo, A. Guagliardi, M. C. Burla, G. Polidori and M. Camalli, *J. Appl. Crystallogr.*, 1994, **27**, 435.
- 36 D. J. Watkin, C. K. Prout, J. R. Carruthers, P. W. Betteridge, CRYSTALS, Issue 10, University of Oxford, Oxford, UK, 1996.
- 37 D. J. Watkin, C. K. Prout and L. J. Pearce, CAMERON, University of Oxford, Oxford, UK, 1996.
- 38 M. J. Frisch, G. W. Trucks, H. B. Schlegel, G. E. Scuseria, M. A. Robb, J. R. Cheeseman, V. G. Zakrzewski, J. A. Montgomery, Jr., R. E. Stratmann, J. C. Burant, S. Dapprich, J. M. Millam, A. D. Daniels, K. N. Kudin, M. C. Strain, O. Farkas, J. Tomasi, V. Barone, M. Cossi, R. Cammi, B. Mennucci, C. Pomelli, C. Adamo, S. Clifford, J. Ochterski, G. A. Petersson, P. Y. Ayala, Q. Cui, K. Morokuma, D. K. Malick, A. D. Rabuck, K. Raghavachari, J. B. Foresman, J. Cioslowski, J. V. Ortiz, B. B. Stefanov, G. Liu, A. Liashenko, P. Piskorz, I. Komaromi, R. Gomperts, R. L. Martin, D. J. Fox, T. Keith, M. A. Al-Laham, C. Y. Peng, A. Nanayakkara, C. Gonzalez, M. Challacombe, P. M. W. Gill, B. Johnson, W. Chen, M. W. Wong, J. L. Andres, C. Gonzalez, M. Head-Gordon, E. S. Replogle and J. A. Pople, GAUSSIAN 98, Revision A.6, Gaussian, Inc., Pittsburgh PA, 1998.
- 39 P. Durand and J. C. Barthelat, *Theor. Chim. Acta*, 1975, **38**, 283.
- 40 Y. Bouteiller, C. Mijoule, M. Nizam, J. C. Barthelat, J. P. Daudey, M. Pelissier and B. Silvi, *Mol. Phys.*, 1988, **65**, 295.